1 # Aerobic H₂ respiration enhances metabolic

2 # flexibility of methanotrophic bacteria

3 **Carlo R. Carere[1,2], Kiel Hards[3], Karen M. Houghton[1], Jean F. Power[1], Ben**

4 **McDonald[2], Christophe Collet[2], Daniel J. Gapes[2], Richard Sparling[4], Gregory M.**

5 **Cook[3], Chris Greening[3,5,6*], Matthew B. Stott[1*]**

6 [1] Extremophile Research Group, GNS Science, Taupō, New Zealand.

7 [2] Scion, Te Papa Tipu Innovation Park, Private Bag 3020, Rotorua, New Zealand.

8 [3] Department of Microbiology and Immunology, University of Otago, New Zealand.

9 [4] Department of Microbiology, University of Manitoba, Canada.

10 [5] Land and Water Flagship, CSIRO, Australia.

11 [6] School of Biological Sciences, Monash University, Australia.

12

13

14 ***Correspondence can be addressed to:**

15 Dr. Chris Greening (chris.greening@monash.au), School of Biological Sciences,
16 Monash University, Clayton VIC 3800, Australia.

17 Dr. Matthew Stott (m.stott@gns.cri.nz), GNS Science, Wairakei Research Centre,
18 114 Karetoto Road, Wairakei, Taupō 3352, New Zealand.

19
20
21
22
23
24
25

Abstract

26

27 Methanotrophic bacteria are important soil biofilters for the climate-active gas

28 methane. The prevailing opinion is that these bacteria exclusively metabolise single-

29 carbon, and in limited instances, short-chain hydrocarbons for growth. This specialist

30 lifestyle juxtaposes metabolic flexibility, a key strategy for environmental adaptation

31 of microorganisms. Here we show that a methanotrophic bacterium from the phylum

32 Verrucomicrobia oxidises hydrogen gas (H_2) during growth and persistence.

33 *Methylacidiphilum* sp. RTK17.1 expresses a membrane-bound hydrogenase to

34 aerobically respire molecular H_2 at environmentally significant concentrations. While

35 H_2 oxidation did not support growth as the sole electron source, it significantly

36 enhanced mixotrophic growth yields under both oxygen-replete and oxygen-limiting

37 conditions and was sustained in non-growing cultures starved for methane. We

38 propose that H_2 is consumed by this bacterium for mixotrophic growth and

39 persistence in a manner similar to other non-methanotrophic soil microorganisms.

40 We have identified genes encoding oxygen-tolerant uptake hydrogenases in all

41 publicly-available methanotroph genomes, suggesting that H_2 oxidation serves a

42 general strategy for methanotrophs to remain energised in chemically-limited

43 environments.

Introduction

44

45 Methane (CH_4) is a potent greenhouse gas with a 100-year global warming potential

46 34 times greater than carbon dioxide (1). Aerobic methane-oxidising bacteria

47 (methanotrophs) constitute the primary biological sink for atmospheric methane (~30

48 Tg annum^{-1}) (2). Together with anaerobic methane-oxidising archaea (ANME), they

49 also capture the majority of biologically- and geologically-produced methane before it

50 enters the atmosphere (3). Relative to their global impact as greenhouse gas

51 mitigators, methanotrophic bacteria exhibit low phylogenetic diversity and are

52 presently limited to 22 genera in the Alphaproteobacteria and Gammaproteobacteria

53 (4), two candidate genera (*Methylacidiphilum* and *Methylacidimicrobium*) in the

54 phylum Verrucomicrobia (5, 6) and two representatives of candidate phylum NC10

55 (7, 8). Methanotrophic bacteria have been isolated from a variety of ecosystems,

56   particularly at the oxic-anoxic interfaces where the fluxes of methane gas are high,

57   including peat bogs, wetlands, rice paddies, forest soils and geothermal habitats (9).

58   Methanotrophic bacteria are classified as obligate aerobes and obligate

59   methylotrophs. They grow by oxidising single carbon or short-chain organic

60   compounds (10). All species oxidise methane to methanol via the soluble or

61   particulate form of methane monooxygenase (sMMO or pMMO respectively).

62   Methanol is then oxidised to carbon dioxide (CO_2), yielding reducing equivalents for

63   energisation of the respiratory chain. The proteobacterial methanotrophs generate

64   biomass by assimilating formaldehyde, a product of MxaFI type methanol

65   dehydrogenase activity, *via* the ribulose monophosphate or serine pathways (2). The

66   verrucomicrobial methanotrophs, in contrast, express an XoxF type methanol

67   dehydrogenase that oxidises methanol directly to formate (11) and generate biomass

68   by fixing CO_2 via the Calvin-Benson-Bassham cycle (12). To remain viable, all

69   methanotrophic bacteria simultaneously require methane, an endogenous reductant

70   (NAD(P)H or quinol), and an exogenous terminal electron acceptor (O_2) to sustain

71   the highly challenging methane monooxygenase reaction ($CH_4 + O_2 + [NAD(P)H +$

72    $H^+]/QH_2 \rightarrow CH_3OH + NAD(P)^+/Q + H_2O$) and to assimilate carbon. This apparently

73   specialist lifestyle is likely to make methanotrophic bacteria highly vulnerable to

74   environmental changes, such as methane-limitation, hypoxia or oxidative stress. But

75   contrary to their apparent metabolic inflexibility, it is known that methanotrophic

76   bacteria are capable of surviving within environments where methane may be

77   limited, variable, or restricted to atmospheric concentrations (1.7 ppmv) (13). Under

78   these conditions low-affinity methane monooxygenase enzymes, which dominate

79   cultivated representatives of methanotrophic bacteria (14), are incapable of methane

80   oxidation and hence other energy sources are required for survival. Recent reports

81   have shown that some methanotrophic bacteria can grow on simple organic acids,

82   alcohols and short-chain alkane gases (15). While this expansion of metabolic ability

83   supersedes the long-held paradigm that methanotrophic bacteria are obligate

84   methylotrophs, these observations are restricted to three of the 24 described

85   methanotrophic genera, *Methylocella, Methylocapsa* and *Methylocystis* (16). It

86   remains unknown whether methanotrophic bacteria more commonly exploit

87   alternative energy sources to survive periods of methane starvation.

88   Recent physiological and ecological studies have collectively shown hydrogen is a

89   widely utilised energy source for microbial growth and survival across a growing

90   range of taxa and soil ecosystems (17-19). The discovery that the dominant soil

91   phyla including Actinobacteria (20) and Acidobacteria (18) can switch from growing

92   on heterotrophic substrates to persisting on atmospheric hydrogen has provided a

93   new understanding of how microorganisms survive nutrient-limited conditions. Given

94   its ubiquity and diffusivity, hydrogen gas is an ideal energy source to support the

95   growth or non-replicative persistence of soil bacteria. Our recent survey of

96   hydrogenase distribution (17), metalloenzymes that catalyse the reversible oxidation

97   of hydrogen, noted that genes encoding hydrogenases were extremely widespread.

98   This result led us to investigate the distribution of hydrogenases in methanotrophic

99   bacteria, and we subsequently identified genes encoding these enzymes in all 31

100 publicly available genomes (Figure S1). This prevalence of hydrogenase genes was

101 surprising given the apparent specialist lifestyle of methanotrophic bacteria. Reports

102 of hydrogenase activity in these microorganisms are scarce. Formate-dependent

103 hydrogen production, under anoxic conditions, has been shown in cultures of

104 *Methylomicrobium album* BG8 and *Methylosinus trichosporium* OB3b (21).

105 *Methylococcus capsulatus* (Bath) is known to express both cytosolic and membrane-

106 bound hydrogenases, though their physiological function has not been resolved (22).

107 The oxidation of hydrogen in methanotrophic bacteria has been predicted to

108 contribute reducing energy for methane oxidation (22), to recycle endogenous

109 hydrogen produced during nitrogen-fixation (23), and to drive the non-productive

110 oxidation of chlorinated solvents (24). However, no studies have confirmed whether

111 hydrogen metabolism contributes to the growth and persistence of these

112 microorganisms.

113 To investigate the physiological role of hydrogenases in methanotrophic bacteria, we

114 undertook a geochemical, molecular and cultivation-based survey of a geothermal

115 soil profile at Rotokawa, New Zealand with known methanotrophic activity (25). In

116 this work, we isolated a thermoacidophilic methanotroph from the genus

117 *Methylacidiphilum* and demonstrate that it oxidises hydrogen gas during both growth

118 and persistence. Hydrogen oxidation occurred through an aerobic respiratory

119 process mediated by a membrane-bound [NiFe]-hydrogenase. Hydrogen oxidation

120 enhanced mixotrophic growth yields during methanotrophic growth, under both

121 oxygen-replete and oxygen-limiting conditions, and was sustained in the absence of

122 methane oxidation. We propose aerobic hydrogen respiration serves as a

123 dependable mechanism for this bacterium – and potentially methanotrophic bacteria

124 in general – to remain energised in otherwise physically-challenging and

125 energetically-variable environments.

126 # Results

127 **Verrucomicrobial methanotrophs are abundant in environments with high**

128 **levels of soil methane and hydrogen oxidation.** A molecular survey of total

129 microbial taxa revealed bacterial and archaeal populations were consistent with

130 acidic soil ecosystems. Methanotrophic verrucomicrobial taxa (family

131 Methylacidiphilaceae) were the dominant OTUs identified at 10 cm depth, accounting

132 for 47 % of all bacterial 16S rRNA gene sequences retrieved (Figure 1a).

133 *Methylacidiphilum* spp. have been previously isolated in acidic geothermal soils in

134 Kamchatka (26), Italy (27, 28) and New Zealand (29) (pH optima of < 3.0), and along

135 with *Methylacidimicrobium* spp. (6), are the only acidophilic methanotrophic bacteria

136 described. At depths between 20-50 cm, Proteobacteria, Actinobacteria and

137 Acidobacteria were present at greater abundance than Verrucomicrobia, none of

138 which include known acidophilic methanotrophs or hydrogenotrophs. At all depths,

139 total microbial taxa were dominated by archaeal OTUs, classified into the order

140 Thermoplasmatales, which is consistent with observations made previously of other

141 acidic geothermal environments (25, 30, 31). Methane and hydrogen soil gas

142 concentrations in this soil embankment were greatest at a depth of 50 cm and

143 steeply decreased below detectable limits by 10 cm depth, suggesting high levels of

144 methane and hydrogen gas oxidation was occurring in shallow depth soils (Figure 1).

145 We consistently observed rapid oxidation of hydrogen and methane in these surface

146 soils when incubated *in vitro* at both mesophilic and thermophilic temperatures

147 (Figure S2). Anticipating soil gas oxidation would primarily be driven by

148 verrucomicrobial methanotrophs, we designed PCR primers targeting the methane

149 monooxygenase and hydrogenase genes encoded in the *Methylacidiphilum*

150 *infernorum* V4 genome (32) (Table S1). qPCR analysis on soil DNA extracts

151 confirmed the genetic capacity of Methylacidiphilaceae to oxidise methane and

152 hydrogen. The abundance of these genes was greatest in the top 20 cm of soil,

153   which corresponded to the zones of the lowest methane and hydrogen soil gas

154   concentrations (Figures 1b & 1c).

155   **Methylacidiphilum sp. RTK17.1 encodes membrane-bound and cytosolic [NiFe]**

156   **hydrogenases.** To gain further insight into the hydrogen-oxidising capacity of the

157   Methylacidiphilaceae within the geothermal soil profile, we isolated, characterised,

158   and sequenced a thermotolerant *Methylacidiphilum* sp. (strain RTK17.1; Table S2)

159   from the Rotokawa soils. Characterisation of *Methylacidiphilum* sp. RTK17.1 showed

160   that it optimally grew at pH 2.5 and 50 °C (T_{max} 58 °C) and could oxidise methane

161   and fix carbon dioxide in common with the reported observations other

162   *Methylacidiphilum* spp. (12). Glycogen accumulation, as previously described in this

163   genus (33), was also observed (data not shown). Analysis of the *Methylacidiphilum*

164   sp. RTK17.1 genome confirmed the basis for these processes (Table S2) and

165   indicated that the metabolic strategy of this strain is consistent with the other

166   verrucomicrobial methanotrophs. Amperometric assays were performed and

167   demonstrated that the isolate oxidised hydrogen gas, providing the first confirmation

168   that *Methylacidiphilum* spp., and indeed members of the dominant soil phylum

169   Verrucomicrobia can metabolise hydrogen. The microorganism rapidly oxidised

170   hydrogen at rates proportional to cell density (Figure 2a) and consumed hydrogen at

171   concentrations as low as 55 ppmv (Figure S3). As with the closely related *M.*

172   *infernorum* V4, we noted the presence of two gene clusters encoding [NiFe]

173   hydrogenases in the sequenced genome (Table S2). These enzymes were classified

174   into Groups 1d (*hyaABC*) and 3b (*hyhBGSL*) based on the criteria of our recent

175   survey on environmental hydrogenase distribution (Figure S1) (17). Group 1d

176   enzymes are membrane-bound, hydrogen-uptake [NiFe] hydrogenases that are

177   believed to yield electrons for aerobic respiration via quinone carriers. In comparison,

178   the identified Group 3b [NiFe] hydrogenase belongs to a class of cytosolic enzymes

179   that couples the oxidation of NADPH to the production of hydrogen (34). Reverse

180   transcription (RT) PCR confirmed *Methylacidiphilum* sp. RTK17.1 constitutively

181   expresses both hydrogenases during methanotrophic growth in the presence of

182   hydrogen (Figure S4).

183   **Methylacidiphilum sp. RTK17.1 oxidises hydrogen in an aerobic respiratory-**

184   **linked process.** Cell lysates targeting the Group 1d hydrogenase efficiently coupled

185   the oxidation of hydrogen to the reduction of the artificial electron acceptor benzyl

186   viologen (E'_o = -374 mV). This activity was localized in the membrane, as shown by

187   the 31-fold increase in benzyl viologen reduction of the membrane fraction relative to

188   the cytosol fraction (Figure 2b). The *hyaC* subunit of this enzyme encodes a

189   predicted membrane-bound *b*-type cytochrome domain known to mediate electron

190   transfer from hydrogen to quinone (35). To probe the physiological interactions of

191   this hydrogenase, we measured real-time hydrogen consumption within cell

192   suspensions. Hydrogen oxidation was stimulated by treatment with the ionophores

193   nigericin and valinomycin respectively (Figures 2c & 2d), showing hydrogenase

194   activity is sensitive to the magnitude of the proton and charge gradients of the

195   proton-motive force. Consistent with being linked to the aerobic respiratory chain,

196   such uncoupled hydrogen oxidation ceased rapidly and could be rescued by

197   supplementation with the terminal electron acceptor, O_2; under these conditions the

198   onset of O_2-limitation was likely exacerbated by the catabolism of endogenous

199   glycogen reserves (Figure S5). By contrast, rates of hydrogen oxidation were

200   reduced following treatment with the protonophore carbonyl cyanide *m*-chlorophenyl

201   hydrazone (CCCP), likely a consequence of secondary intracellular acidification

202   (Figure S6). The Group 1d [NiFe] hydrogenase mediating this process appears

203   oxygen-tolerant, a finding consistent with the sequenced small subunit gene

204   encoding a 6Cys[4Fe3S] cluster, which rapidly reactivates hydrogenases following

205   oxygen inhibition (36, 37). Collectively, these findings demonstrate that this

206   hydrogenase is a strictly membrane-bound, respiratory-linked, oxygen-dependent

207   enzyme that drives ATP synthesis through the Knallgas reaction, i.e. by

208   chemiosmotically coupling hydrogen oxidation to oxygen reduction.

209   **Oxidation of hydrogen enhances mixotrophic growth**. Pure culture experiments

210   with *Methylacidiphilum* sp. RTK17.1 were performed to determine the physiological

211   roles of the Group 1d hydrogenase. We observed that methane and hydrogen were

212   co-oxidised in both batch bioreactor cultures (Figure S7) and chemostat experiments

213   (Table 1). In these experiments, an exogenous energy source (i.e. hydrogen or

214   methane) was always supplied in excess to suppress the induction of endogenous

215   metabolism and prevent glycogen catabolism (38). Chemostat experiments revealed

216   that hydrogen oxidation is stimulated under hypoxic growth conditions. Observed

217   rates of hydrogen oxidation were 77-fold greater when cells were oxygen-limited

218 compared to oxygen excess conditions (Table 1). Further, under oxygen-limiting

219 conditions with 1.9 % hydrogen addition, the specific consumption rate of hydrogen

220 was 42 % greater than observed rates of methane oxidation. Hydrogen addition into

221 the feedgas significantly (*p*-value < 0.05) increased growth yields (g_{CDW} mol_{CH4}^{-1}) of

222 *Methylacidiphilum* sp. RTK17.1 by 33 % under oxygen excess and 51 % under

223 oxygen-limited conditions (Table 1). Additionally, cellular growth yields (as

224 determined by total protein) of *Methylacidiphilum* sp. RTK17.1, following one week

225 incubation in the presence of 1 % hydrogen and 10 % methane (v/v), were

226 significantly greater than when grown exclusively on methane in batch experiments

227 (Figure S3b). Hydrogen oxidation was also observed both in methane-starved

228 cultures of *Methylacidiphilum* sp. RTK17.1 and following the addition of 4 % (v/v)

229 acetylene (Figure S3a), an inhibitor of methane monooxygenase activity (39). Hence,

230 while hydrogen oxidation alone cannot sustain growth of this methanotroph, it

231 appears sufficient to maintain both the proton-motive force and ATP synthesis

232 required for long-term survival in the absence of the methylotrophic growth

233 substrates.

Discussion

235 This study shows a methanotrophic bacterium is able to constitutively consume

236 methane and hydrogen, either together or separately depending on gas availability,

237 to meet energy needs. We demonstrated that the genetic determinants of aerobic

238 hydrogen respiration, specifically genes encoding a member of the Group 1d [NiFe]

239 hydrogenases, are encoded and expressed in the verrucomicrobial methanotroph

240 *Methylacidiphilum* sp. RTK17.1. The strain rapidly oxidised exogenous hydrogen

241 with this enzyme in a membrane-bound aerobic respiratory process and likely

242 provides hydrogen-derived reducing equivalents to the quinone pool for methane

243 monooxygenase activity and/or cytochrome reduction, *via* activity of a recently

244 described alternative (ACIII) cytochrome complex (40). Our model of how methane,

245 methanol and hydrogen oxidation are integrated into the respiratory chain of

246 verrucomicrobial methanotrophs is shown in Figure 3. Through this metabolic

247 flexibility, we propose that *Methylacidiphilum* sp. RTK17.1 is able to balance the

248 catabolic and anabolic requirements for reducing energy imposed by its challenging

249 methanotrophic lifestyle and the methane monooxygenase reaction. This flexibility

250 likely contributes to the dominance of the Methylacidiphilaceae in aerated acidophilic

251 geothermal soils at Rotokawa, New Zealand. As a dominant genus in the uppermost

252 20 cm of these soils, *Methylacidiphilum* sp. RTK17.1 can simultaneously oxidise

253 geothermally-produced methane and hydrogen gases while consuming atmospheric

254 oxygen and fixing carbon dioxide and nitrogen gases. In addition to conferring a

255 survival advantage during periods of methane limitation, our data shows hydrogen

256 oxidation may be favoured during hypoxia. When grown under oxygen-limiting

257 conditions, rates of hydrogen consumption in cultures of *Methylacidiphilum* sp.

258 RTK17.1 increased by 77-fold and exceeded observed rates of methane oxidation

259 (Table 1). Similarly, a transcriptome study investigating nitrogen fixation reported that

260 the Group 1d hydrogenase in *Methylacidiphilum fumarolicum* SolV was upregulated

261 20-fold in response to oxygen limitation (41). This preference for hydrogen suggests

262 methanotrophic bacteria occupying the soil oxic/anoxic interface display a

263 predominately mixotrophic lifestyle. In fact, under oxygen limited experimental

264 conditions, up to 32 % of the total reducing energy supplied to the respiratory chain

265 may be provided from hydrogen-derived electrons. Recalling that pMMO requires

266 oxygen as a substrate to catalyse the conversion of methane to methanol,

267 mixotrophy through hydrogen respiration both sustains the energy requirements for

268 cell growth while reducing the overall demand for oxygen. Given the energetic

269 requirement for cell maintenance is three orders of magnitude less than for growth

270 (42, 43), it is probable that hydrogen oxidation serves as a reliable mechanism for

271 the persistence of methanotrophic bacteria in these habitats.

272 Genomic evidence supports that hydrogen oxidation is a commonly utilised strategy

273 for the growth and survival of methanotrophic bacteria. Hydrogenases were identified

274 in all 31 genomes of methanotrophic bacteria surveyed (Figure S1). Previous studies

275 have shown two model methanotrophs, *Methylosinus trichsporium* OB3b (21) and

276 *Methylococcus capsulatus* (Bath) (24), oxidise hydrogen but the physiological role of

277 their encoded hydrogenases has never been fully investigated. Consistent with

278 hydrogen contributing to the persistence of methanotrophic bacteria, genes encoding

279 the Group 1h [NiFe] hydrogenases, while absent from *Methylacidiphilum* sp.

280 RTK17.1, were identified in the genomes of selected alphaproteobacterial and

281 verrucomicrobial methanotrophs. These high-affinity enzymes are capable of

282 oxidising tropospheric concentrations of hydrogen and have been linked to

283 persistence within the dominant soil phyla Actinobacteria (20) and Acidobacteria

284 (18). Our genomic analysis indicates methanotrophic bacteria may additionally

285 evolve hydrogen fermentatively (*via* Group 3b and 3d [NiFe] hydrogenases), which

286 by analogy with *Mycobacterium smegmatis*, may be important for surviving anoxia

287 (34). They also encode the capacity to sense hydrogen (*via* Group 2b and 2c [NiFe]

288 hydrogenases) which may serve to regulate expression of uptake hydrogenases and

289 also potentially global cellular processes. Hydrogen is likely an attractive energy

290 source for these microorganisms because of its high-diffusibility, relative

291 dependability, and high energy content. Whereas biogenic methane is exclusively

292 produced by methanogenic archaea, hydrogen is biologically produced by diverse

293 organisms across the three domains of life as a result of fermentation,

294 photobiological processes, and nitrogen fixation (17). Hence, the ability of

295 methanotrophic bacteria to utilise this widespread energy source may enhance their

296 capacity to colonise environments and adapt to environmental change. This hidden

297 metabolic flexibility may explain why the range of low-affinity methanotrophic

298 bacteria extends beyond ecosystems with high methane fluxes (44).

299 By demonstrating that respiratory-linked hydrogen oxidation enhances growth, we

300 reveal that verrucomicrobial methanotrophs are mixotrophs capable of growth and

301 survival on hydrocarbon and non-hydrocarbon substrates alike. The narrative that

302 methanotrophic bacteria are niche specialists, with obligately methylotrophic

303 lifestyles, is based on studies under optimal growth conditions and ignores the

304 requirement of these organisms to adapt to methane and/or oxygen limitation.

305 Particularly within dynamic oxic/anoxic boundaries, where methanotrophic bacteria

306 occur in high abundance (45), a specialist metabolism is likely to reduce the overall

307 fitness of these microorganisms. We therefore propose that mixotrophic growth and

308 survival through hydrogen metabolism provides a general mechanism by which this

309 contradiction is resolved. Expanding the metabolic flexibility of methanotrophs will

310 have broad ecological implications and result in an improved understanding of global

311 methane and hydrogen cycles.

312

313

Methods

314

Environmental sampling. Soil samples (~ 50 g) were collected every 10 cm from

the surface of the sampling site (38°37'30.8"S, 176°11'55.3"E) to a maximum depth

of 50 cm. This site, located within Rotokawa geothermal field was selected on the

basis of previous research showing elevated soil gas concentrations (25). Soil

temperatures were measured in the field using a 51II single input digital thermometer

(Fluke). The pH was measured upon returning to the laboratory using a model

HI11310 pH probe (Hanna Instruments). Soil gas samples were collected every 10

cm using a custom built gas-sampling probe equipped with a 1 l gas tight syringe

(SGE Analytical Science). Gas samples were collected and stored at 25 °C in 50 ml

Air & Gas Sampling Bags (Calibrated Instruments) and were processed within 48 h

on a 490 MicroGC (Agilent Technologies, Santa Clara, CA) equipped with Molecular

Sieve 5A with heated injector (50 °C, back-flush at 5.10 s, column at 90 °C, 150

kPa), a PoraPak Q column with heated injector (50 °C, no back-flush, column at 70

°C,150 kPa) and a 5CB column with heated injector (50 °C, no back-flush, column at

80 °C, 150 kPa). Methane and hydrogen gas consumption by soil microbial

communities was determined by incubating 1 g of soils collected from the Rotokawa

sampling site (depth < 10 cm) in 112 ml gas-tight serum bottles at 37 and 50 °C. The

serum bottle headspace were air emended with 300 ppmv and 400 ppmv of

hydrogen and methane gas respectively. Headspace methane and hydrogen gas

concentrations were measured with a PeakPerformer gas chromatograph equipped

with a flame ionising detector (FID: methane) and a PP1 Gas Analyzer equipped with

a reducing compound photometer (RCP: hydrogen).

Isolation and cultivation of *Methylacidiphilum* sp. RTK17.1. Soil samples (1 g)

were inoculated into serum bottles containing 50 ml media (pH 2.5). All cultivations

were performed in a V4 mineral medium as described previously (29) but with the

addition of rare earth elements lanthanum and cerium (27). Methane (10 % v/v) and

carbon dioxide (1 %) were added to an air headspace and samples were incubated

at 60 °C with shaking 150 rpm. Methane in the headspace was monitored with a

PeakPerformer gas chromatograph equipped with a flame ionising detector (FID).

Following several passages (10 % v/v) into liquid media, enrichments were

transferred onto solid media. Following several weeks incubation (60 °C) single

346 colonies were re-streaked before being transferred back into liquid media. Isolate

347 identity was confirmed via sequencing of the 16S rRNA gene (Macrogen) using

348 bacterial 9f/1492r primers (46).

349 **Chemostat cultivation and batch experiments.**

350 Chemostat cultivation of *Methylacidiphilum* sp. RTK17.1 was performed to

351 investigate the influence of hydrogen on growth under oxygen excess and oxygen-

352 limiting conditions. A 1 l bioreactor (BioFlo 110, New Brunswick Scientific. Edison,

353 NJ, USA) was used for these studies. Cultures were incubated at 50 °C and pH 3

354 with continuous stirring (800 rpm). Bioreactor volume was kept constant at 0.5 l by

355 automatic regulation of the culture level. V4 mineral media was supplied at a

356 constant flow rate of 10 ml h^{-1} (D=0.02 h^{-1}). Dissolved oxygen was monitored using a

357 InPro 6810 Polarographic Oxygen Sensor (Mettler-Toledo). Custom gas mixtures

358 were prepared in a compressed gas cylinder and supplied to the chemostat at a rate

359 of 10 ml min^{-1} using a mass flow controller (EL-FLOW, Bronkhorst, Netherlands).

360 Gas mixtures contained approximately (v/v) 3 % methane and 26 % carbon dioxide

361 for all experiments. For oxygen excess and oxygen-limiting conditions, (v/v) 14.1 %

362 and 3.5 % oxygen was supplied. High, medium and low hydrogen experiments

363 consisted of (v/v) 1.9 %, 0.7 % and 0.4 % hydrogen additions. The balance of all gas

364 mixtures was made up with nitrogen.

365 Cell density in liquid samples was monitored by measuring turbidity at 600 nm using

366 a Ultrospec 10 cell density meter (Amersham Bioscience). One unit of OD_{600} was

367 found to be equivalent to 0.43 g l^{-1} cell dry weight (CDW) for *Methylacidiphilum* sp.

368 RTK17.1. After achieving a steady state condition as determined by OD_{600}, influent

369 and effluent gas concentrations were monitored over several days using a 490

370 MicroGC (Agilent Technologies, Santa Clara, CA). Biomass cell dry weight was used

371 to calculate growth rate and specific gas consumption rate.

372 To investigate whether *Methylacidiphilum* sp. RTK17.1 oxidises ecologically

373 significant concentrations of hydrogen, 350 ml cultures (in triplicate) were incubated

374 in 1 l rubber-stoppered Schott bottles in a headspace of air supplemented with 100-

375 250 ppmv hydrogen, 1 % (v/v) methane and 1 % carbon dioxide. Acetylene gas was

376 added in some experiments (4 % v/v) to inhibit MMO activity as previously described

377 (39). Finally, to determine if growth was enhanced in the presence of hydrogen, 20

378 paired cultures (n = 40) of *Methylacidiphilum* sp. RTK17.1 were incubated with or

379 without 1 % (v/v) hydrogen in an air headspace supplemented with (v/v) 10 %

380 methane and 1 % carbon dioxide. Cultures were incubated in a custom Test Tube

381 Oscillator (TTO; agitation 1.2 Hz; Terratec). Following seven days incubation, total

382 protein was determined as described previously (47). Statistical significance of

383 observed differences of growth yields was determined using a *student's t-test* (α =

384 0.05). Headspace mixing ratios of hydrogen and methane were monitored

385 throughout batch experiments as described above.

386 **Hydrogenase activity measurements.** Hydrogenase activity of *Methylacidiphilum*

387 sp. RTK17.1 was measured in stationary-phase cultures harvested from the

388 bioreactor. For amperometric measurements, whole-cells were concentrated 5-, 10-,

389 20-, and 30-fold by centrifugation followed by resuspension in phosphate-buffered

390 saline (pH 7.4). Rate of hydrogen oxidation was measured at 50 °C using a

391 hydrogen-MR hydrogen microsensor (Unisense) as previously described (18, 48).

392 For colourimetric assays, 500 ml culture was harvested by centrifugation (15 min,

393 5,000 × g, 4 °C) and treated as previously described (18, 20) to prepare crude,

394 cytosolic and membrane fractions for analysis. To test for hydrogenase activity,

395 samples (20 µg protein) from each cell fraction were incubated with 1 ml 50 mM

396 potassium phosphate buffer (pH 7.0) and 50 µM benzyl viologen for eight hours in an

397 anaerobic chamber (5 % hydrogen, 10 % carbon dioxide, 85 % nitrogen (v/v)).

398 Debris was removed by centrifugation (15 min, 10,000 × g, 4 °C) and the

399 absorbance of the supernatants was read at 604 nm in a Jenway 6300

400 spectrophotometer.

401 Additional methodologies for nucleic acid extraction, PCR, genome sequencing,

402 oxygen consumption experiments and soil microbial community determination can

403 be found in the supporting information.

References

405 1. Shindell, D.T.*, et al.* Improved attribution of climate forcing to emissions. *Science*. **326**(5953),
406   716-718 (2009).
407 2. Hanson, R.S. & Hanson, T.E. Methanotrophic bacteria. *Microbiol Rev* **60**(2), 439-471 (1996).

3.   Oremland, R.S. & Culbertson, C.W. Importance of methane-oxidizing bacteria in the methane budget as revealed by the use of a specific inhibitor. *Nature.* **356**(6368), 421-423 (1992).

4.   Euzeby, J.P. List of Bacterial Names with standing in nomenclature: a folder available on the Internet. *Int J Syst Bacteriol.* **47**(2), 590-592 (1997).

5.   Op den Camp, H.J.M.*, et al.* Environmental, genomic and taxonomic perspectives on methanotrophic Verrucomicrobia. *Environ Microbiol Rep.* **1**(5), 293-306 (2009).

6.   van Teeseling, M.C.*, et al.* Expanding the verrucomicrobial methanotrophic world: description of three novel species of Methylacidimicrobium gen. nov. *Appl Environ Microbiol* **80**(21), 6782-6791 (2014).

7.   Ettwig, K.F.*, et al.* Nitrite-driven anaerobic methane oxidation by oxygenic bacteria. *Nature.* **464**(7288), 543-548 (2010).

8.   Haroon, M.F.*, et al.* Anaerobic oxidation of methane coupled to nitrate reduction in a novel archaeal lineage. *Nature.* **500**(7464), 567-570 (2013).

9.   Singh, B.K., Bardgett, R.D., Smith, P. & Reay, D.S. Microorganisms and climate change: terrestrial feedbacks and mitigation options. *Nat Rev Micro.* **8**(11), 779-790 (2010).

10. Dedysh, S.N., Knief, C. & Dunfield, P.F. Methylocella species are facultatively methanotrophic. *J Bacteriol.* **187**(13), 4665-4670 (2005).

11. Keltjens, J.T., Pol, A., Reimann, J. & Op den Camp, H.J.M. PQQ-dependent methanol dehydrogenases: rare-earth elements make a difference. *Appl Microbiol Biotechnol.* **98**(14), 6163-6183 (2014).

12. Khadem, A.F.*, et al.* Autotrophic methanotrophy in Verrucomicrobia: Methylacidiphilum fumariolicum SolV uses the Calvin-Benson-Bassham cycle for carbon dioxide fixation. *J Bacteriol.* **193**(17), 4438-4446 (2011).

13. Kolb, S., Knief, C., Dunfield, P.F., & Conrad, R. Abundance and activity of uncultured methanotrophic bacteria involved in the consumption of atmospheric methane in two forest soils. *Environ Microbiol.* **7**(8), 1150-1161 (2005).

14. Ho, A.*, et al.* Conceptualizing functional traits and ecological characteristics of methane-oxidizing bacteria as life strategies. *Environ Microbiol Rep.* **5**(3), 335-345 (2013).

15. Crombie, A.T. & Murrell, J.C. Trace-gas metabolic versatility of the facultative methanotroph Methylocella silvestris. *Nature.* **510**(7503), 148-151 (2014).

16. Semrau, J.D., DiSpirito, A.A., & Vuilleumier, S. Facultative methanotrophy: false leads, true results, and suggestions for future research. *FEMS Microbiol Lett.* **323**(1), 1-12 (2011).

17. Greening C.*, et al.* Genomic and metagenomic surveys of hydrogenase distribution indicate H_2 is a widely utilised energy source for microbial growth and survival. *ISME J.* **10**, 761-777 (2015).

18. Greening, C.*, et al.* Persistence of the dominant soil phylum Acidobacteria by trace gas scavenging. *Proc Natl Acad Sci USA.* **112**(33), 10497-10502 (2015).

19. Greening, C. & Cook, G.M. Integration of hydrogenase expression and hydrogen sensing in bacterial cell physiology. *Curr Opin Microbiol.* **18**, 30-38 (2014).

20. Greening, C., Berney, M., Hards, K., Cook, G.M., & Conrad, R. A soil actinobacterium scavenges atmospheric H_2 using two membrane-associated, oxygen-dependent [NiFe] hydrogenases. *Proc Natl Acad Sci USA.* **111**(11), 4257-4261 (2014).

21. Kawamura, S., O'Neil, J.G., & Wilkinson, J.F. Hydrogen production by Methylotrophs under anaerobic conditions. *J ferment technol.* **61**(2), 151-156 (1983).

22. Hanczar, T., Csaki, R., Bodrossy, L., Murrell, J.C., & Kovacs, K.L. Detection and localization of two hydrogenases in Methylococcus capsulatus (Bath) and their potential role in methane metabolism. *Arch Microbiol.* **177**(2), 167-172 (2002).

23. Ward, N.*, et al.* Genomic insights into methanotrophy: The complete genome sequence of Methylococcus capsulatus (Bath). *PLoS Biol.* **2**(10), e303 (2004).

24. Shah, N.N., Hanna, M.L., Jackson, K.J., & Taylor, R.T. Batch cultivation of Methylosinus trichosporium OB3B: IV. Production of hydrogen-driven soluble or particulate methane monooxygenase activity. *Biotechnol Bioeng.* **45**(3), 229-238 (1995).

25. Sharp, C.E.*, et al.* Distribution and diversity of Verrucomicrobia methanotrophs in geothermal and acidic environments. *Environ Microbiol.* **16**(6), 1867-1878 (2014).

26. Islam, T., Jensen, S., Reigstad, L.J., Larsen, O. & Birkeland, N.K. Methane oxidation at 55 degrees C and pH 2 by a thermoacidophilic bacterium belonging to the Verrucomicrobia phylum. *Proc Natl Acad Sci USA*. **105**(1), 300-304 (2008).

27. Pol, A.*, et al.* Rare earth metals are essential for methanotrophic life in volcanic mudpots. *Environ Microbiol* **16**(1), 255-264 (2014).

28. van Teeseling, M.C.F.*, et al.* Expanding the verrucomicrobial methanotrophic world: description of three novel species of Methylacidimicrobium gen. nov. *Appl Environ Microbiol.* **80**(21), 6782-6791 (2014).

29. Dunfield, P.F.*, et al.* Methane oxidation by an extremely acidophilic bacterium of the phylum Verrucomicrobia. *Nature.* **450**(7171), 879-882 (2007).

30. Golyshina, O.V. Environmental, biogeographic, and biochemical patterns of Archaea of the family Ferroplasmaceae. *Appl Environ Microbiol.* **77**(15), 5071-5078 (2011).

31. Inskeep, W.P.*, et al.* The YNP metagenome project: Environmental parameters responsible for microbial distribution in the Yellowstone geothermal ecosystem. *Front Microbiol.* **4**,67 (2013).

32. Hou, S.*, et al.* Complete genome sequence of the extremely acidophilic methanotroph isolate V4, Methylacidiphilum infernorum, a representative of the bacterial phylum Verrucomicrobia. *Biology Direct.* **3**, 26-26 (2008).

33. Khadem, A.F.*, et al.* Genomic and physiological analysis of carbon storage in the verrucomicrobial methanotroph "Ca. Methylacidiphilum fumariolicum" SolV. *Front Microbiol.* **3**, 345 (2012).

34. Berney, M., Greening, C., Conrad, R., Jacobs, W.R., & Cook, G.M. An obligately aerobic soil bacterium activates fermentative hydrogen production to survive reductive stress during hypoxia. *Proc Natl Acad Sci USA.* **111**(31), 11479-11484 (2014).

35. Volbeda, A.*, et al.* Crystal Structure of the O_2-tolerant membrane-bound hydrogenase 1 from Escherichia coli in complex with its cognate cytochrome b. *Structure.* **21**(1), 184-190 (2013).

36. Fritsch, J., Lenz, O. & Friedrich, B. Structure, function and biosynthesis of O_2-tolerant hydrogenases. *Nat Rev Micro.* **11**(2), 106-114 (2013).

37. Shomura, Y., Yoon, K-S., Nishihara, H. & Higuchi, Y. Structural basis for a [4Fe-3S] cluster in the oxygen-tolerant membrane-bound [NiFe]-hydrogenase. *Nature.* **479**(7372), 253-256 (2011).

38. Russell, J.B. & Cook, G.M. Energetics of bacterial growth: balance of anabolic and catabolic reactions. *Microbiol Rev.* **59**(1), 48-62 (1995).

39. Bédard, C. & Knowles, R. Physiology, biochemistry, and specific inhibitors of CH_4, NH_4^+, and CO oxidation by methanotrophs and nitrifiers. *Microbiol Rev.* **53**(1), 68-84 (1989).

40. Refojo, P.N., Sousa, F.L., Teixeira, M. & Pereira, M.M. The alternative complex III: A different architecture using known building modules. *BBA – Bioenergetics.* **1797**(12), 1869-1876 (2010).

41. Khadem, A.F., Pol, A., Wieczorek, A.S., Jetten, M.S.M., & Op den Camp, H.J.M. Metabolic regulation of "Ca. Methylacidiphilum fumariolicum" SolV cells grown under different nitrogen and oxygen limitations. *Front Microbiol.* **3**, 266 (2012).

42. Biddle, J.F.*, et al.* Heterotrophic Archaea dominate sedimentary subsurface ecosystems off Peru. *Proc Natl Acad Sci USA.* **103**(10), 3846-3851 (2006).

43. Price, P.B. & Sowers, T. Temperature dependence of metabolic rates for microbial growth, maintenance, and survival. *Proc Natl Acad Sci USA.* **101**(13), 4631-4636 (2004).

508 44. Dedysh, S.N., Panikov, N.S. & Tiedje, J.M. Acidophilic methanotrophic communities from
509   Sphagnum peat bogs. *Appl Environ Microbiol.* **64**(3), 922-929 (1998).
510 45. Crevecoeur, S., Vincent, W.F., Comte, J. & Lovejoy, C. Bacterial community structure across
511   environmental gradients in permafrost thaw ponds: methanotroph-rich ecosystems. *Front*
512   *Microbiol.* **6**(192), 1-15 (2015).
513 46. Weisburg, W.G., Barns, S.M., Pelletier, D.A. & Lane, D.J. 16S ribosomal DNA amplification for
514   phylogenetic study. *J Bacteriol.* **173**(2), 697-703 (1991).
515 47. Bradford, M.M. Rapid and sensitive method for quantitation of microgram quantities of
516   protein utilizing principle of protein-dye binding. *Anal Biochem.* **72**, 248-254 (1976).
517 48. Berney, M., Greening, C., Hards, K., Collins, D. & Cook, G.M. Three different [NiFe]
518   hydrogenases confer metabolic flexibility in the obligate aerobe Mycobacterium smegmatis.
519   *Environ Microbiol.* **16**(1), 318-330 (2014).
520 49. Chin, C-S*, et al.* Nonhybrid, finished microbial genome assemblies from long-read SMRT
521   sequencing data. *Nat Meth.* **10**(6), 563-569 (2013).
522 50. Markowitz, V.M., *et al.* IMG: the integrated microbial genomes database and comparative
523   analysis system. *Nucleic Acids Res.* **40**(D1), D115-D122 (2012).
524 51. Edgar, R.C. UPARSE: highly accurate OTU sequences from microbial amplicon reads. *Nat*
525   *Methods.* **10**(10), 996-998 (2013).
526 52. Wang, Q., Garrity, G.M., Tiedje, J.M. & Cole, J.R. Naive Bayesian classifier for rapid
527   assignment of rRNA sequences into the new bacterial taxonomy. *Appl Environ Microbiol.*
528   **73**(16), 5261-5267 (2007).
529 53. McDonald, D*., et al.* An improved Greengenes taxonomy with explicit ranks for ecological
530   and evolutionary analyses of bacteria and archaea. *ISME J.* **6**(3), 610-618 (2012).
531 54. Caporaso, J.G*., et al.* Ultra-high-throughput microbial community analysis on the Illumina
532   HiSeq and MiSeq platforms. *ISME J.* **6**(8), 1621-1624 (2012).
533 55. Klindworth, A*., et al.* Evaluation of general 16S ribosomal RNA gene PCR primers for classical
534   and next-generation sequencing-based diversity studies. *Nucleic Acids Res.* **41**(1):e1 (2013).
535

Acknowledgments

549

Author contributions

CRC, CG, MBS, GC, KMH, KH, CC, DJG, RS and BM contributed to experimental design. Bioreactor and wet lab experiments were conducted by CRC, BM, CC, DJG and KMH. CRC, CG and KH undertook cell respiratory analysis. CRC and MBS performed fieldwork and genomic analyses. JFP performed the microbial community analysis. CRC, MBS, CG, KH and GC wrote the manuscript.

Competing Interests

The authors declare no competing financial interests.

Figures and Tables
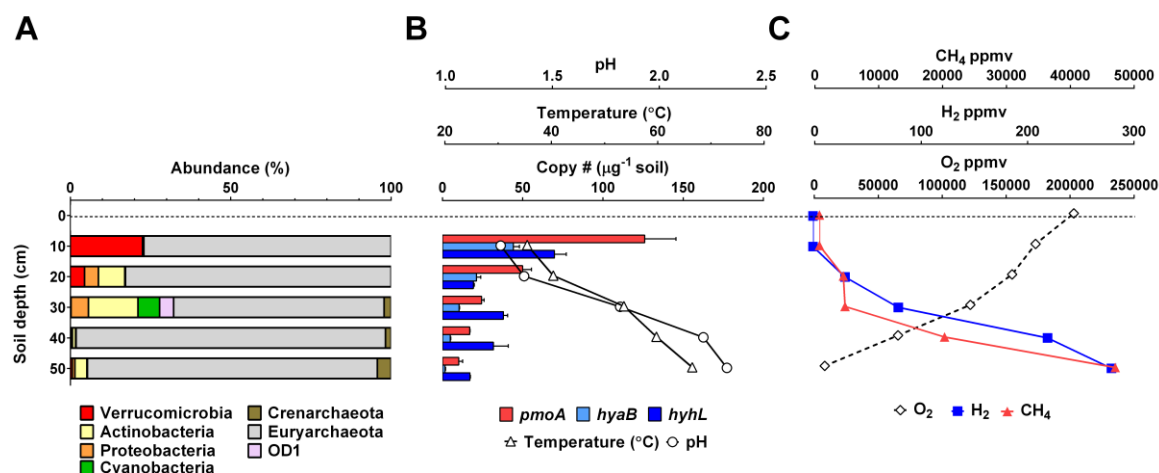
Figure 1. Methanotrophic bacteria are highly abundant in the uppermost soils in Rotokawa, New Zealand. OTUs classified belonging to phylum Verrucomicrobia were the dominant bacterial taxa identified in the top 10 cm. Consistent with a methanotrophic lifestyle, all verrucomicrobial OTUs were further classified into the family Methylacidiphilaceae. 16S rRNA gene sequencing was performed (illumina) on total DNA extracted at 10-50 cm soil depth. Non-rarefied abundance results (%) are shown for all OTUs (> 100 reads) from 130,289 total sequence reads (with an average of 26,058 per sample depth). The abundance (B) of the verrucomicrobial particulate methane monooxygenase (*pmoA*), Group 1d (*hyaB*) and Group 3b (*hyhL*) hydrogenase genes and corresponding (C) soil gas, temperature and pH profiles suggests both high levels of aerobic methane and hydrogen oxidation activity by these acidophilic taxa in the uppermost 20 cm. Error bars shown represent the standard deviation of triplicate measurements.

573
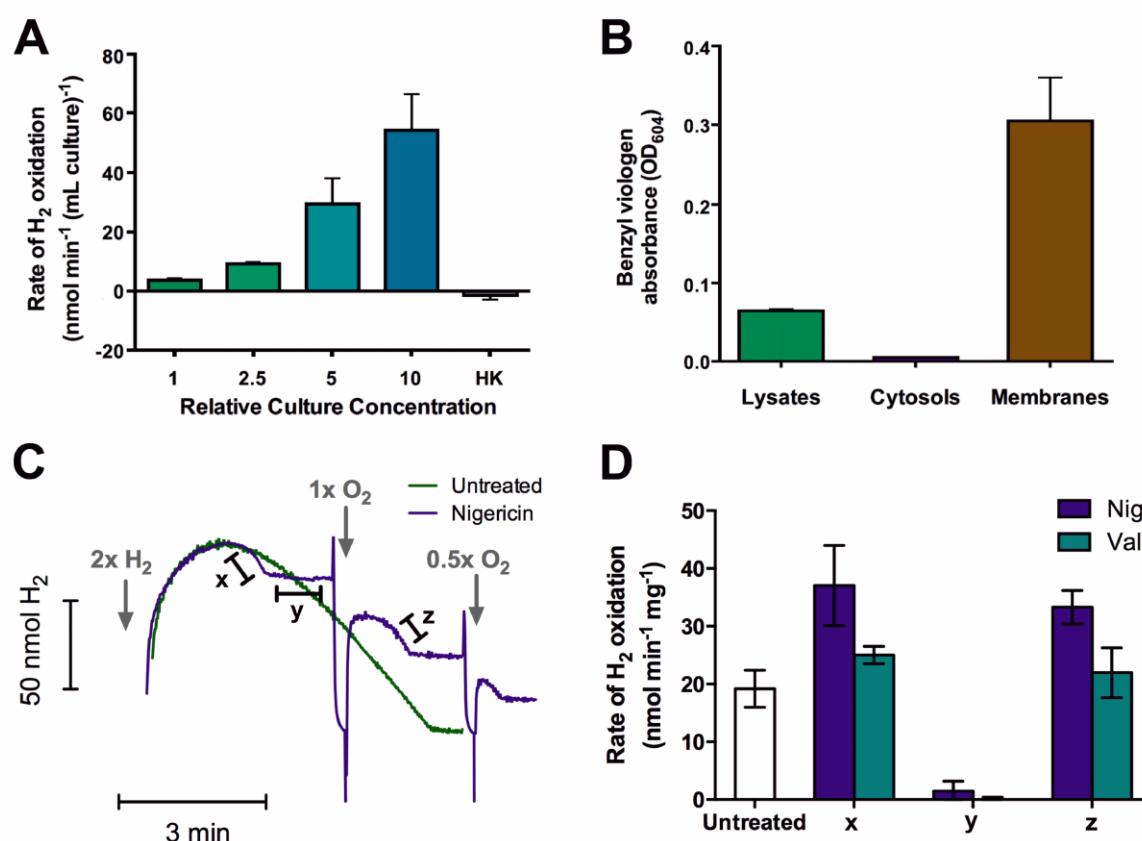
Figure 2. Hydrogenase activity of *Methylacidiphilum* sp. RTK17.1. (A) Whole-cell oxidation of hydrogen measured amperometrically using a hydrogen microsensor. The density-dependence of this process and its sensitivity to heat inactivation (HK) is shown. (B) Colourimetric detection of hydrogenase activity in protein concentration-normalized cell lysates, cytosols, and membranes anaerobically treated with the artificial electron acceptor benzyl viologen. (C) Real-time hydrogen oxidation by untreated cells and nigericin-treated cells. The relative amounts of hydrogen and oxygen added at specific time points is shown. (D) Rates of hydrogen oxidation of untreated, nigericin-treated, and valinomycin-treated cells. For the uncoupler-treated cultures, the initial (*x*), oxygen-limited (*y*), and oxygen restored (*z*) rates of oxidation are shown, which correspond to the rates highlighted in panel (C). Endogenous glycogen catabolism likely contributed to oxygen-limitation (y) observed in nigericin treated cells (Figure S5).

587

588
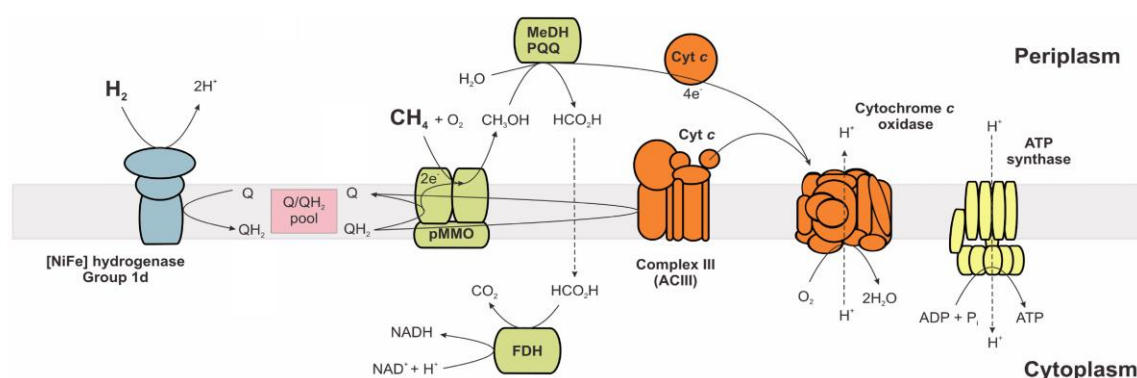
Figure 3. Proposed model of respiratory-linked methane and hydrogen oxidation in *Methylacidiphilum* sp. RTK17.1. During mixotrophic growth, the oxidation of both hydrogen (H_2) and methane (CH_4) yields reducing equivalents (QH_2) for the respiratory chain, a large proton-motive force is generated, and sufficient ATP is produced for growth via an H^+-translocating F_1F_o-ATP synthase. Some of the quinol generated through H_2 oxidation provides the electrons necessary for pMMO catalysis. Following CH_4 oxidation by pMMO, ensuing reactions catalysed by an XoxF type methanol dehydrogenase (MeDH) and formate dehydrogenase (FDH) contribute additional reductant (Cyt *c* and NADH) into the respiratory chain for ATP production and growth (11). In methane-limiting conditions, the identified Group 1d [NiFe] hydrogenase generates a small proton-motive force, oxidised reductant (Q) is maintained via type ACIII cytochrome complex (40) and sufficient ATP is generated for maintenance. Respiratory complexes I and II are not shown but are encoded in the genome of *Methylacidiphilum* sp. RTK17.1 (Table S2).

603

Table 1. Hydrogen oxidation by *Methylacidiphilum sp.* RTK17.1 during chemostat cultivation.

605

Condition [a,b]	Growth rate	H$_2$ consumption		CH$_4$ consumption		Biomass Yield[d]
	(mg l^{-1} h^{-1})	(mmol l^{-1} h^{-1})	(mmol g$_{CDW}$$^{-1}$ h^{-1})	(mmol l^{-1} h^{-1})	(mmol g$_{CDW}$$^{-1}$ h^{-1})	(g$_{CDW}$ mol$_{CH4}$$^{-1}$)
O$_2$ excess, medium H$_2$	9.33 (± 0.52)	0.01 (± 0.01)	0.01 (± 0.03)	1.06 (± 0.12)	2.40 (± 0.38)	8.90[Ŧ] (± 1.51)
O$_2$ excess, no H$_2$	8.17 (± 0.82)	0.00	0.00	1.22 (± 0.05)	2.85 (± 0.18)	6.68 (± 0.41)
O$_2$-limiting, high H$_2$	5.57 (± 0.16)	0.78 (± 0.02)	2.66 (± 0.11)	0.55 (± 0.03)	1.89 (± 0.11)	10.11[¥] (± 0.64)
O$_2$-limiting, medium H$_2$	4.99 (± 0.17)	0.33 (± 0.01)	1.34 (± 0.06)	0.70 (± 0.02)	2.80 (± 0.13)	7.16 (± 0.34)
O$_2$-limiting, low H$_2$	5.60 (± 0.31)	0.19 (± 0.00)	0.73 (± 0.04)	0.71 (± 0.01)	2.68 (± 0.16)	7.87[¥] (± 0.45)
O$_2$-limiting, no H$_2$	5.40 (± 0.26)	0.00	0.00	0.80 (± 0.05)	3.11 (± 0.27)	6.79 (± 0.55)

606

[a] Feedgas was continuously supplied at a rate of 10 ml min^{-1} with the following composition % (v/v): O$_2$ Excess, 14.1 %; O$_2$ limiting, 3.5 %. High, medium and low H$_2$ experiments consisted of 1.9 %, 0.7 % and 0.4 % H$_2$ supply. For all experiments excess CH$_4$ was supplied at 3 %, CO$_2$ at 26 % with the balance made up with N$_2$.

[b] a dilution rate of 0.02 h^{-1} was maintained for all experiments

[c] gram cell dry weight (g$_{CDW}$) measurements were determined by correlating OD$_{600}$ measurements to an existing standard curve (OD$_{600}$ = 1 corresponds to 0.43 g$_{CDW}$/l).

[d] Standard deviation shown in brackets are calculated from a minimum of triplicate measurements

[¥] denotes significant increase (*p*-value < 0.05) in yield from O$_2$-limiting, no H$_2$ result; unpaired *t*-test, one tailed.

[Ŧ] denotes significant increase (*p*-value < 0.05) in yield from O$_2$ excess, no H$_2$ result; unpaired *t*-test, one tailed.

Supporting Information

Supplementary Methods

Nucleic acid extraction

Methylacidiphilum sp. RTK17.1 genomic DNA was extracted using the NucleoSpin Tissue kit (Macherey-Nagel) as per the manufacturer's instructions for difficult to lyse Gram-positive bacteria. DNA was extracted from Rotokawa soil samples using the NucleoSpin Soil DNA extraction kit (Macherey-Nagel) as per the manufacturers recommended protocol.

For RNA isolation from *Methylacidiphilum* sp. RTK17.1, stationary phase (Abs_{600nm} = 4.0, 10 ml cultures) cells were harvested by centrifugation (27,000 × g, 20 min, 4 °C), resuspended in 1 ml RNA Later (ThermoFisher Scientific) and stored at -20 °C as recommended. Cell lysis, total RNA extractions and cDNA synthesis were performed as previously described (18).

PCR, RT-PCR, Quantitative PCR and genome sequencing

Methylacidiphilum sp. RTK17.1 genomic DNA and cDNA (10 ng) was (RT)PCR amplified using i-Taq DNA polymerase (2.5 U; Intron Biotechnology) in 50 μl reactions containing dNTPs (1 mM), 1X PCR Buffer, $MgCl_2$ (1.5 mM), forward primer (0.5 μM) and reverse primer (0.5 μM). Amplifications conditions using an Mx3000p thermocycler (Strategene) were as follows; an initial 94 °C for 5 min; followed by 30 cycles of 94 °C for 45 s; 55 °C for 45 s; 72 °C for 90 s; and a final extension at 72 °C for 5 min. PCRs were run through electrophoresis on a 1 % (w/v) TAE agarose gel with 1X RedSafe nucleic acid staining solution and visualised on a GeneGenius Bio Imaging System (Syngene).

Quantitative-PCR (qPCR) was performed to investigate the abundance of Verrucomicrobial methanotrophs type by probing for MMO (*pmoA)* and hydrogenase genes (Group 1d and 3b) within the Rotokawa soil profile. Total DNA extracted from 1 g soil was amplified using a Probe Fast Universal qPCR kit (KAPA Biosystems) according to the manufacturer's instructions. Primer sequences for all qPCR amplifications are provided in Table S2. qPCR reactions were optimised and

645   conducted on an Mx3000p thermocycler (Strategene). Abundance (expressed per µg

646   Soil) of MMO and hydrogenase genes in DNA samples was calculated from cycle

647   threshold values (Ct) and standard curves.

648   To prepare qPCR standard curves, amplicons were cloned following the

649   recommended protocol for the TOPO-TA Cloning kit (ThermoFisher Scientific).

650   Transformation of competent *Eschericia coli* cells was achieved using a MicroPulse

651   electroporator (BioRad) at setting EC1. Standard curves for qPCR were prepared

652   from the serial dilution of plasmid DNA recovered using the Zippy Plasmid Miniprep

653   kit (Zymo Research) following Qubit fluorometirc quantification (ThermoFisher

654   Scientific).

655   The genome of *Methylacidiphilum* sp. RTK17.1 was sequenced using the PacBio RS

656   platform (Macrogen). Genome assembly was performed, *de novo*, via the SMRT

657   Portal using hierarchical genome-assembly process (HGAP) pipeline (49). A high

658   quality *de novo* assembly was generated from three SMRT sequencing runs the

659   HGAP.3 protocol. A pre-assembly genome construct was assembled using Celera

660   Assembler and then polished using Quiver (49). Quality assessment of the *de novo*

661   assembly was conducted using BridgeMapper. Gene prediction was performed using

662   Quiver and genome annotation was completed using the integrated microbial

663   genomes database pipeline (50).

664   **Soil microbial community determination**

665   The V4 region of the 16S rRNA gene was sequenced using the Illumina MiSeq®

666   System. Sequences were analysed using UPARSE pipeline for quality filtering and

667   clustering (51). Briefly, paired end reads were merged and those less than 200 or

668   350 bp were discarded, for 515f/806r and 341/785r primer amplicons respectively

669   (Table S1). Quality filtering was applied with a maximum expected error value of 1.

670   Retained sequences were dereplicated and unique sequences removed. Next, reads

671   were clustered to 97 % similarity, which includes a chimera check, and a *de novo*

672   database was created of representative operational taxonomic units (OTUs). Original

673   pre-filtered sequences were mapped to these OTUs, and taxonomy was assigned

674   using the Ribosomal Database Project classifier (with a minimum confidence score

675   of 0.5) (52) against the GreenGenes 16S rRNA database (13_8 release) (53). Final

676 count number was 130,289 reads across all depths for the 515f/806r primer set, with

677 a total of 48 differential OTUs (492,588 for 341/785r, with 107 OTUs).

678 **Static liquid fed-batch bioreactor cultivations**

679 *Methylacidiphilum* sp. RTK17.1 was cultivated to stationary phase for subsequent

680 hydrogenase activity and oxygen respiration measurements in a semi-continuous

681 fed-batch bioreactor (New Brunswick; volume 1l, pH control 2.5, temp 50 °C,

682 agitation 100 rpm) in an artificial headspace composed of 10 % methane, 10 %

683 hydrogen, 2 0 % O_2, 40 % carbon dioxide (v/v, balance N_2; flow rate 60 ml min^{-1})

684 equipped with headspace recirculation and automated sampling via a 490 MicroGC

685 (Agilent Technologies, Santa Clara, CA). Gas mixtures were supplied for 2 min every

686 hour at a rate of 60 ml min^{-1}.

687 **Oxygen consumption experiments.**

688 Oxygen consumption experiments were performed on cell suspensions of

689 *Methylacidiphilum* sp. RTK17.1 to determine the influence of endogenous glycogen

690 catabolism on O_2 dependent hydrogenase measurements. For these experiments, 2

691 mL cells (OD_{600} 1.0) were added to a Clarke-type oxygen electrode and incubated at

692 50 °C for up to 12 min without the addition of exogenous energy sources. Cell

693 suspensions were treated with the protonophore (1 μM) CCCP, 1 mM Iodoacetamide

694 (an inhibitor of glycolysis) and 1 mM potassium cyanide (KCN) to determine whether

695 observed rates oxygen consumption were a consequence of glycogen catabolism.

696 **Figure S1.** The classification and phylogeny of the [NiFe] hydrogenase large subunit identified in the genomes of methanotrophic

697 bacteria.

698
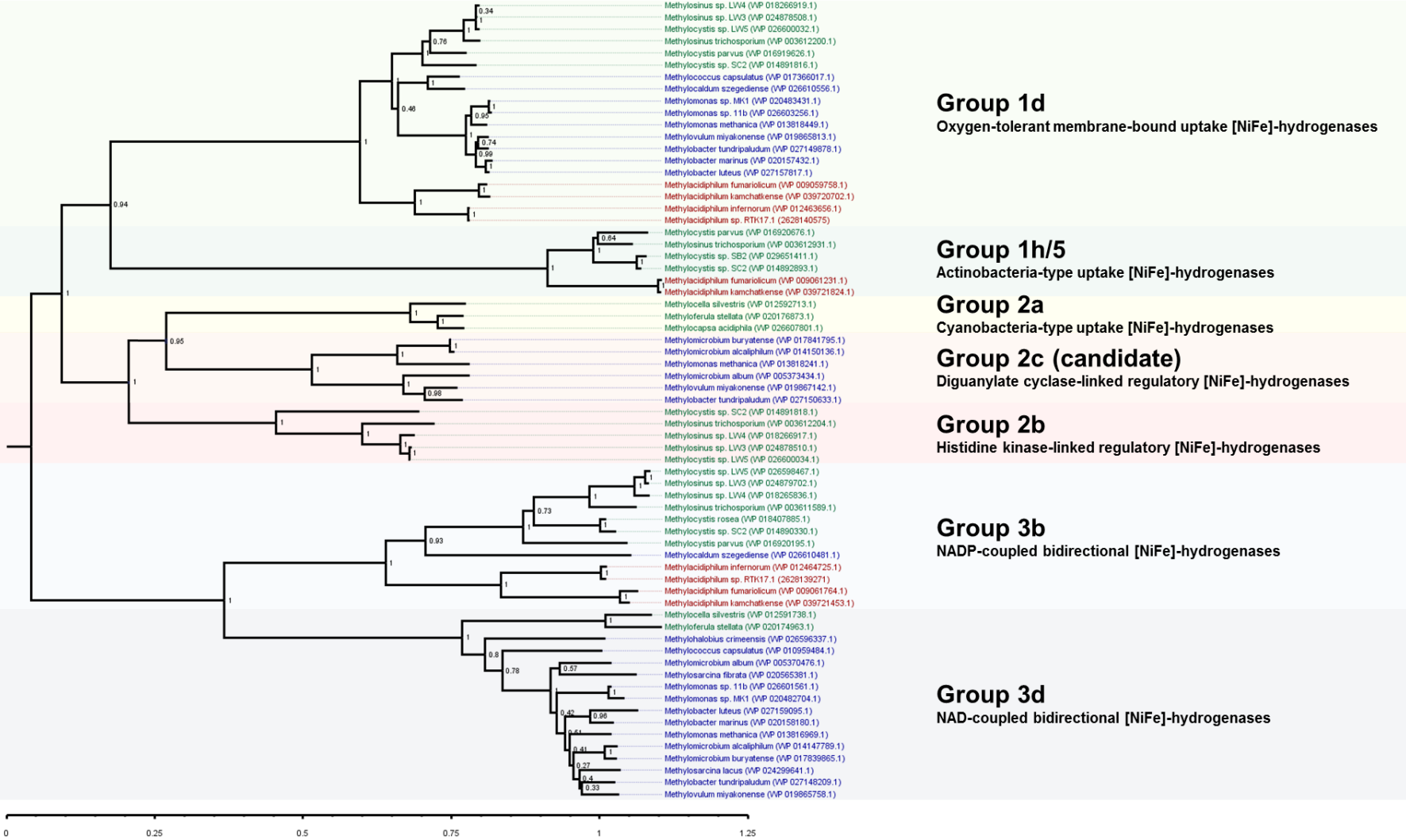
699   **Figure S2.** Oxidation of CH_4 and H_2 by surface Rotokawa soils (< 10 cm depth)

700   incubated at mesophilic (37 °C) and thermophilic (50 °C) temperatures. Soils

701   samples (1 g) were collected and incubated following addition of A) ~400 ppmv CH_4

702   and B) ~300 ppmv H_2 into the headspace. The average and standard deviation of

703   triplicate samples is shown.

704
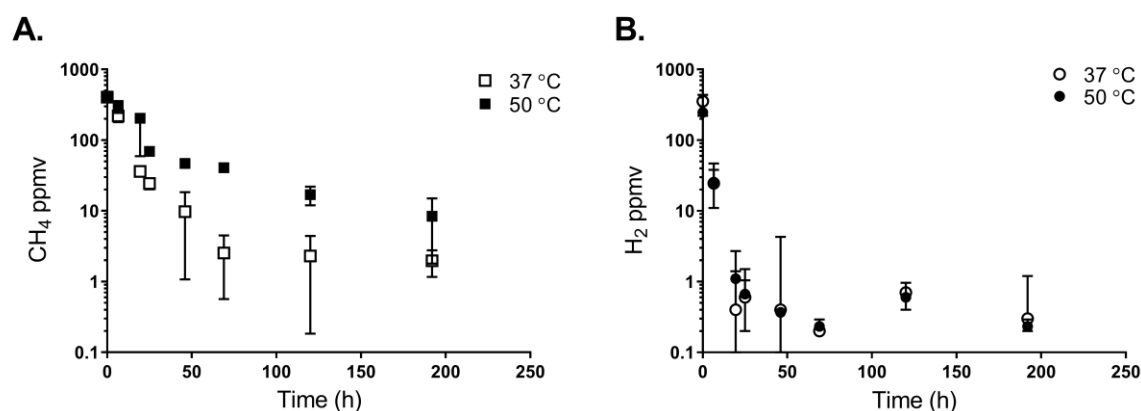
705 **Figure S3.** Batch culture growth experiments and observations of methane and

706 hydrogen oxidation for *Methylacidiphilum* sp. RTK17.1 following treatment with

707 acetylene. (A) Rates of hydrogen oxidation are greatest during methanotrophic

708 growth (red circle) but are also measurable in the presence of 4 % (v/v) acetylene

709 gas (an inhibitor of pMMO; green triangle) and in the absence of methane (blue

710 square). Black triangles with dashed lines denote negative controls. Observed rates

711 of methane and hydrogen oxidation decline as substrates are exhausted. Error bars

712 shown represent the standard deviation of biological triplicate samples. (B)

713 Methanotrophic growth of *Methylacidiphilum* sp. RTK17.1 is enhanced by the

714 addition of 1 % H_2 (v/v). Differences in growth observed (as determined by total

715 protein) with and without hydrogen addition were analysed following 1 week

716 incubation (50 °C) in 20 paired samples by one-tailed t-test assuming Gaussian

717 distribution and determined to be significant (*p-value* 0.007, *df*= 19, SEM error bars

718 are shown).

719
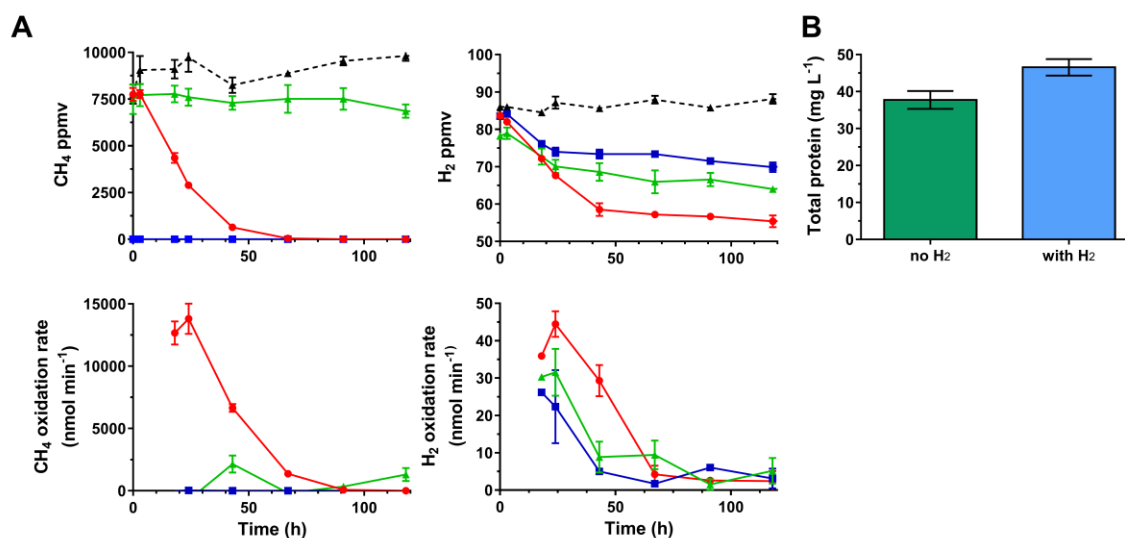
720 **Figure S4.** Reverse Transcriptase PCR of total mRNA isolated from stationary

721 phase cultures of *Methylacidiphilum* RTK17.1 confirms the expression of the

722 membrane bound Group 1d [NiFe] hydrogenase. Only faint amplification of cDNA

723 encoding the cytosolic Group 3b enzyme was observed.

724

725
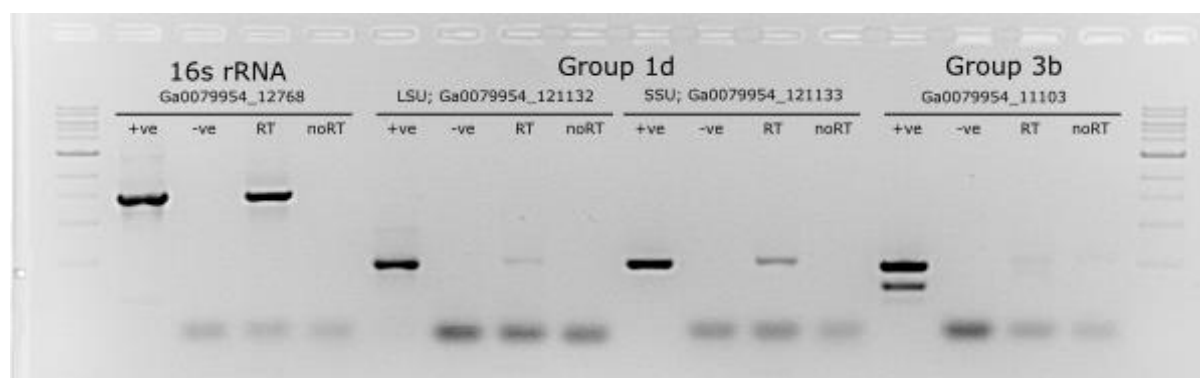
726 **Figure S5.** Treatment of cell suspensions of *Methylacidiphilum sp.* RTK17.1 with the

727 uncoupler carbonyl cyanide *m*-chlorophenyl hydrazone (CCCP), the glycolytic

728 inhibitor iodoacetamide (IAA) and the respiratory chain inhibitor potassium cyanide

729 (KCN). This indicates that observed oxygen consumption, in the absence of

730 exogenous energy sources (H_2 or CH_4), is likely a consequence of endogenous

731 glycogen catabolism.

732

733
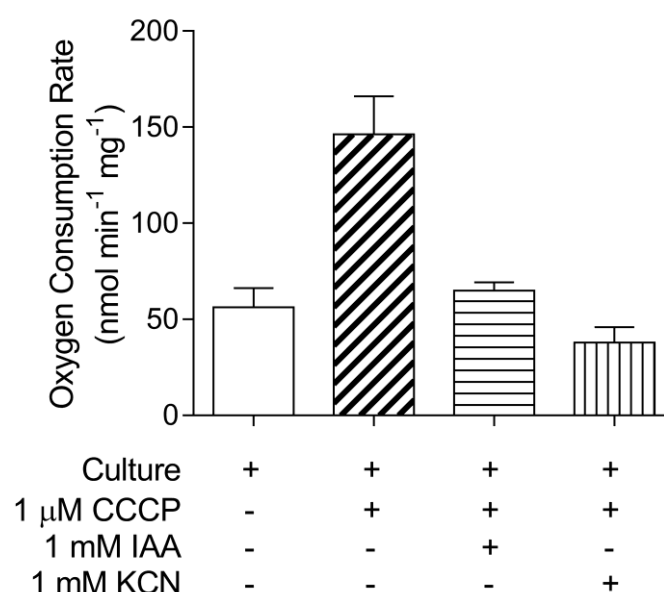
734 **Figure S6.** Treatment of concentrated cell suspensions of *Methylacidiphilum sp.*

735 RTK17.1 with the ionophores nigericin (Nig) and valinomycin (Val) indicates

736 hydrogenase activity is sensitive to the magnitude of the proton- and charge-

737 gradients of the proton-motive force. The reduction in rate of hydrogen oxidation

738 observed when treated with carbonyl cyanide *m*-chlorophenyl hydrazone (CCCP) is

739 likely a consequence of secondary intracellular acidification.

740

Figure S7. *Methylacidiphilum* sp. RTK17.1 oxidises hydrogen (H_2) and fixes carbon dioxide (CO_2) in the absence of methane (CH_4). In static liquid fed-batch bioreactor experiments, stationary-phase cultures were incubated (50 °C) in a nitrogen headspace with mixing ratios (v/v) as follows: (A) 0 % CH_4, 9 % H_2, 19 % CO_2, 20 % O_2; (B): 9 % CH_4, 0 % H_2, 19 % CO_2, 20 % O_2; (C): 9 % CH_4, 9 % H_2, 19 % CO_2, 20 % O_2. In the absence of CH_4 or H_2 addition, Argon (10 %) supplementation was used to maintain equivalent headspace mixing ratios of the other gases between experiments. We did not determine whether CO_2 fixation in the absence of CH_4 was driven by H_2 oxidation or instead metabolism of endogenous glycogen reserves.

750
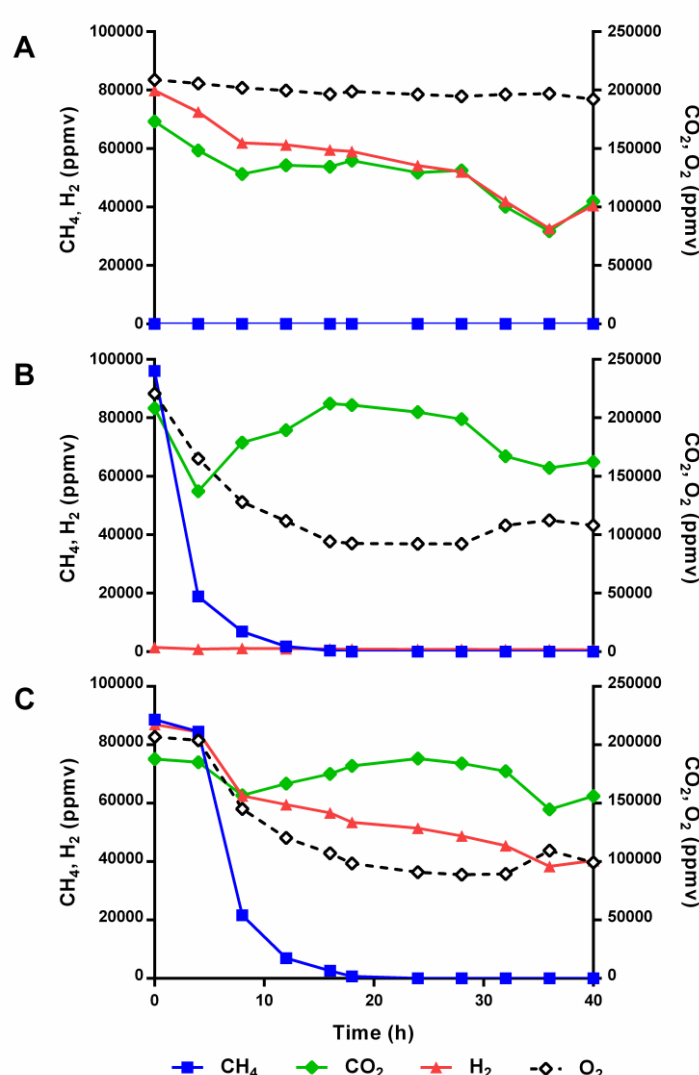
751 **Table S1.** Primers used for qPCR analysis targeting the methane monooxygenase and hydrogenases of *Methylacidiphilum* spp.

752

Target	Locus	Amplicon size (bp)	Primer name	Sequence	References
hyd1d	Minf_1320	187	qMinf_1320_fwd	TGCACCTGACACAAATGGTT	This study
	Minf_1320		qMinf_1320_rvs	TGCTTCAGTCGATTTTGCAC	
hyd3b	Minf_2390	241	qMinf_2390_fwd	CCTGGAAGAAGAGCTGTTGG	This study
	Minf_2390		qMinf_2390_rvs	ACTTTCCAGGGAGGCAAAAT	
pmoA	Minf_1507	208	qMinf_1507_fwd	ACTTCGTTGTGACCGCTCTT	This study
	Minf_1507		qMinf_1507_rvs	GCAAAGCTTCTCATCGTTCC	
pmoA	Minf_1510	172	qMinf_1510_fwd	AGAACTTTGGGGTTGGCTTT	This study
	Minf_1510		qMinf_1510_rvs	CCTCATCGTTCCCGTTTCTA	
pmoA	Minf_1590	202	qMinf_1590_fwd	CGCATATGCTTTTGCTTTGA	This study
	Minf_1590		qMinf_1590_rvs	CGGTCCTAAAGCTCCTCCTT	
16S rRNA		1483	9f	GAGTTTGATCMTGGCTCAG	(46)
			1492r	TACCTTGTTACGACTT	
16S rRNA		291	Uni515f	GTGYCAGCMGCCGCGGTAA	(54)
			Uni806r	GGACTACNVGGGTWTCTAAT	
16S rRNA		444	Bac341f	CCTACGGGNGGCWGCAG	(55)
			Bac785r	GACTACHVGGGTATCTA ATCC	

753 **Table S2.** Genes involved in one-carbon and hydrogen metabolism, as well as
754 glycogen storage and utilization in *Methylacidiphilum* sp. RTK17.1. Amino acid
755 orthologs to *Methylacidiphilum infernorum* V4 are shown.

Gene	Predicted Function	Gene ID *	*M. infernorum* ortholog	% ID
Methane oxidation to methanol				
pmoC1	particulate methane monooxygenase, C subunit	KU509367	WP_012463847.1	99
pmoA1	particulate methane monooxygenase, A subunit	KU509368	ABX56601.1	100
pmoB1	particulate methane monooxygenase, B subunit	KU509369	WP_012463845.1	99
pmoC2	particulate methane monooxygenase, C subunit	KU509373	WP_048810233.1	99
pmoA2	particulate methane monooxygenase, A subunit	KU509371	WP_012463843.1	99
pmoB2	particulate methane monooxygenase, B subunit	KU509372	WP_012463842.1	99
pmoC2	particulate methane monooxygenase, C subunit	KU509370	WP_012463844.1	99
pmoC3	particulate methane monooxygenase, C subunit	KU509318	WP_012463927.1	99
pmoA3	particulate methane monooxygenase, A subunit	KU509319	WP_012463926.1	99
pmoB3	particulate methane monooxygenase, B subunit	KU509320	WP_012463925.1	97
Methanol oxidation to formate (11)				
xoxF	methanol dehydrogenase, large subunit	KU509410	WP_012463329.1	99
xoxJ[#]	unknown function, involved in methanol oxidation	Ga0079954_12828	WP_012463332.1	99
mxaB	transcriptional regulator	KU509376	WP_012463785.1	100
moxY	methanol utilization control sensor protein	KU509377	WP_012463784.1	100
mxaR	ATPase involved in methanol oxidation	KU509402	WP_012463503.1	97
no homologs of *mxaI mxaS mxaA mxaC mxaK mxaL mxaD mxaE mxaH mxaW mxaG*				
Tetrahydrofolate synthesis				
folK	2-amino-4-hydroxy-6-hydroxymethyldihydropteridine diphosphokinase	KU509446	WP_048810035.1	97
folP	dihydropteroate synthase	KU509345	WP_012464234.1	99
folP	dihydropteroate synthase	KU509478	WP_048810563.1	98
folC	bifunctional folylpolyglutamate synthase/dihydrofolate synthase	KU509444	WP_012462725.1	99
Formate oxidation to CO_2				
fdsG	formate dehydrogenase, gamma subunit	KU509398	WP_048810187.1	97
fdsB	formate dehydrogenase, beta subunit	KU509399	WP_012463566.1	100
fdsA	formate dehydrogenase, alpha subunit	KU509400	WP_048810186.1	99

fdsD	formate dehydrogenase delta subunit	KU509401	WP_048810185.1	94
hpr	formate dehydrogenase	KU509384	WP_012463659.1	99
ehrB	putative formate-dependent oxidoreductase complex subunit	KU509439	WP_012462850.1	99
ehrD	putative formate-dependent oxidoreductase complex subunit	KU509438	WP_012462851.1	99
ehrF	putative formate-dependent oxidoreductase complex subunit	KU509436	WP_012462853.1	99
ehrA	putative formate-dependent oxidoreductase complex subunit	KU509437	WP_012462852.1	99
ehrE	putative formate-dependent oxidoreductase complex subunit	KU509449	WP_012462854.1	100
ehrG	putative formate-dependent oxidoreductase complex subunit	KU509435	WP_048810433.1	97
Methylamine oxidation genes				
mauB	methylamine dehydrogenase large subunit	KU509332	WP_012464333.1	98
mauE	methylamine utilization protein	KU509331	WP_012464334.1	99
mauD	methylamine utilization protein	KU509330	WP_012464335.1	100
mauA#	methylamine dehydrogenase small subunit	Ga0079954_121718	WP_048810312.1	99
mauG	methylamine utilization protein, cytochrome c peroxidase	KU509329	ACD84055.1	99
no homologs of *mauF mauC mauJ mauL mauM mauN*				
Hydrogen metabolism				
hyaF	hydrogenase-1 operon protein	KU509388	WP_012463654.1	99
hyaC	oxygen-tolerant membrane-bound [NiFe] - hydrogenase, cytochrome *b* subunit	KU509387	WP_012463655.1	99
hyaB	oxygen-tolerant membrane-bound [NiFe] hydrogenase, large subunit	KU509386	WP_012463656.1	99
hyaA	oxygen-tolerant membrane-bound [NiFe] hydrogenase, small subunit	KU509385	WP_048810203.1	99
hyhB	NADP-coupled cytosolic bidirectional hydrogenase, FeS subunit	KU509477	WP_012464721.1	99
crp	cyclic nucleotide-binding domain-containing protein	KU509476	WP_012464722.1	97
hyhG	NADP-coupled cytosolic bidirectional hydrogenase, diaphorase subunit NAD(P)H-flavin reductase	KU509475	WP_012464723.1	98
hyhS	NADP-coupled cytosolic bidirectional hydrogenase, small subunit	KU509474	WP_012464724.1	98
hyhL	NADP-coupled cytosolic bidirectional hydrogenase, large subunit	KU509473	WP_012464725.1	98
hypB	hydrogenase maturase protein, Ni storage	KU509355	WP_012464135.1	99
hypC	hydrogenase maturase protein, Fe- $(CN^-)_2$ - CO insertion	KU509357	WP_012464132.1	100
hypD	hydrogenase maturase protein, Fe- $(CN^-)_2$ - CO insertion	KU509358	WP_012464131.1	99
hypE	hydrogenase maturase protein, CN^- ligand biosynthesis	KU509359	WP_012464130.1	99

hypF	hydrogenase maturase protein, CN⁻ ligand biosynthesis	KU509356	WP_012464133.1	99
Copper homeostasis				
cueR	copper resistance operon regulatory protein	KU509440	WP_012462789.1	99
copA	Cu(I)-translocating P-type ATPase/ multicopper oxidase, copper-binding site	KU509375	gb|ABX56608.1|	99
cueO	multicopper oxidase family protein	KU509374	WP_048810228.1	99
cusA	copper efflux pump	KU509461	WP_012462437.1	99
cusB#	copper efflux pump membrane fusion protein	Ga0079954_11259	WP_012462436.1	98
cusS	copper sensor histidine kinase	KU509433	WP_012462941.1	99
cusR	DNA binding copper response regulator	KU509432	WP_048810437.1	99
Coenzyme PQQ synthesis				
pqqB	coenzyme PQQ synthesis protein B	KU509397	WP_012463570.1	99
pqqC	coenzyme PQQ synthesis protein C	KU509396	WP_012463571.1	99
pqqD	coenzyme PQQ synthesis protein D	KU509395	WP_048810188.1	98
pqqD	coenzyme PQQ synthesis protein D	KU509434	WP_012462864.1	97
pqqE	coenzyme PQQ synthesis protein E	KU509394	WP_048810189.1	99
No homologs of *pqqG pqqF pqqA*				
Glycogen synthesis				
mdoG	glycans biosynthesis protein	KU509364	WP_012463952.1	98
mdoG	glycans biosynthesis protein	KU509365	WP_012463951.1	99
	glucan elongaton module (mdoH-like)	KU509366	WP_048810251.1	99
GH57	glycosyl hydrolase family 57	KU509382	WP_012463665.1	99
amyA	alpha amylase, catalytic domain	KU509383	WP_012463664.1	98
glgA	glycogen synthase	KU509360	WP_012464092.1	99
glgA	glycogen synthase (ADP-glucose)	KU509479	WP_048810560.1	98
glgB	1,4-alpha-glucan branching enzyme	KU509409	WP_012463357.1	99
glgC	glucose-1-phosphate adenylyltransferase	KU509460	WP_048810004.1	99
glgP	starch phosphorylase	KU509451	WP_012462597.1	99
glgP	starch phosphorylase	KU509431	WP_012462995.1	99
glgP	starch phosphorylase	KU509429	WP_012463128.1	99
gdb1	glycogen debranching enzyme (alpha-1,6-glucosidase)	KU509417	WP_012463227.1	99
rfaG	glycosyltransferase	KU509418	WP_012463226.1	99
glcD	glycolate oxidase	KU509414	WP_048810142.1	98
glcD	glycolate oxidase FAD binding subunit	KU509413	WP_012463233.1	98
aceB	malate synthase	KU509415	WP_012463229.1	98
aceA	isocitrate lyase	KU509416	WP_048810457.1	98
manB	phosphoglucomutase	KU509328	WP_012464463.1	99
Calvin-Benson Cycle				
cbbS	ribulose 1,5-bisphosphate carboxylase, small subunit	KU509390	WP_012463599.1	98
cbbL	ribulose 1,5-bisphosphate carboxylase, large subunit	KU509389	WP_012463600.1	99
cbbX	probable Rubsico expression protein CbbX	KU509391	WP_012463598.1	99

pgk	phosphoglycerate kinase	KU509406	WP_048810158.1	98
gapA	glyceraldehyde-3-phosphate dehydrogenase	KU509405	WP_012463370.1	99
fbaA	putative fructose-bisphosphate aldolase	KU509327	WP_048810542.1	98
fbaA2	fructose-bisphosphate aldolase, class II	KU509448	WP_012462629.1	100
fbp	fructose-1,6-bisphosphatase I	KU509361	WP_012464020.1	99
glpX	fructose-1,6-bisphosphatase II	KU509381	WP_012463695.1	100
tktB	transketolase	KU509393	WP_012463596.1	99
xfp	xylulose-5-phosphate/fructose-6-phosphate phosphoketolase	KU509412	WP_012463240.1	99
tpiA	triosephosphate isomerase	KU509407	WP_012463368.1	98
rpiB	ribose 5-phosphate isomerase B	KU509459	WP_012462539.1	99
prkB	phosphoribulokinase	KU509392	WP_012463597.1	100
rpe	ribulose-phosphate 3-epimerase	KU509354	WP_012464174.1	99

TCA cycle

gltA	citrate synthase	KU509447	WP_012462674.1	99
acnA	aconitate hydratase	KU509408	WP_012463364.1	99
icd	isocitrate dehydrogenase	KU509411	WP_012463276.1	99
sucA	2-oxoglutarate dehydrogenase, E1 component	KU509464	WP_048810403.1	98
sucB	2-oxoglutarate dehydrogenase, E2 component, dihydrolipoamide succinyltransferase	KU509463	WP_012462410.1	98
lpdA	pyruvate/2-oxoglutarate dehydrogenase, E3 component, dihydrolipoamide dehydrogenase	KU509462	WP_012462411.1	99
lpdA	pyruvate/2-oxoglutarate dehydrogenase, E3 component, dihydrolipoamide dehydrogenase	KU509362	WP_012463971.1	98
sucD	succinyl-CoA synthetase subunit alpha	KU509403	WP_012463383.1	99
sucC	succinyl-CoA synthetase subunit beta	KU509404	WP_048810162.1	99
sdhB	succinate dehydrogenase, catalytic subunit	KU509442	WP_012462728.1	99
sdhA	succinate dehydrogenase, flavoprotein subunit	KU509441	WP_012462729.1	98
sdhC	succinate dehydrogenase, cytochrome b subunit	KU509443	WP_012462727.1	98
fumC	fumarase	KU509428	WP_012463130.1	100
mdh	malate dehydrogenase	KU509380	WP_048810212.1	99

ATP Synthase

atpD	F-type H$^+$-transporting ATPase subunit beta	KU509426	WP_048810122.1	99
atpC	F-type H$^+$-transporting ATPase subunit epsilon	KU509425	WP_012463177.1	99
	ATP synthase protein I	KU509424	WP_012463178.1	98
atpB	ATP synthase F0 subcomplex A subunit	KU509423	WP_012463179.1	98
atpE	F-type H$^+$-transporting ATPase subunit c	KU509422	WP_012463180.1	98
atpF	ATP synthase F0 subcomplex B subunit	KU509421	WP_012463181.1	99

atpA	F-type H+-transporting ATPase subunit alpha	KU509420	WP_012463182.1	99
atpG	F-type H+-transporting ATPase subunit gamma	KU509419	WP_012463183.1	100
atpH	F-type H$^+$-transporting ATPase subunit delta	KU509469	WP_012464754.1	99
atpB	F-type H$^+$-transporting ATPase subunit a	KU509472	WP_012464751.1	99
atpE	F-type H$^+$-transporting ATPase subunit c	KU509471	WP_012464752.1	100
atpF	F-type H$^+$-transporting ATPase subunit b	KU509470	WP_048810391.1	99
atpA	F-type H$^+$-transporting ATPase subunit alpha	KU509468	WP_012464755.1	99
atpG	F-type H$^+$-transporting ATPase subunit gamma	KU509467	WP_012464756.1	99
atpD	F-type H$^+$-transporting ATPase subunit beta	KU509466	WP_012464757.1	100
atpC	F-type H$^+$-transporting ATPase subunit epsilon	KU509465	WP_012464758.1	100
NADH dehydrogenase				
nuoB	NADH-quinone oxidoreductase subunit B	KU509458	WP_012462551.1	99
nuoA	NADH-quinone oxidoreductase subunit A	KU509480	WP_012464634.1	99
nuoC	NADH-quinone oxidoreductase subunit C	KU509457	WP_012462552.1	100
nuoD	NADH-quinone oxidoreductase subunit D	KU509456	WP_012462553.1	99
nuoE	NADH-quinone oxidoreductase subunit E	KU509455	WP_012462554.1	99
nuoF	NADH-quinone oxidoreductase subunit F	KU509454	WP_012462555.1	99
nuoG	NADH-quinone oxidoreductase subunit G	KU509453	WP_012462556.1	99
nuoH	NADH-quinone oxidoreductase subunit H	KU509452	WP_012462557.1	99
nuoI	NADH-quinone oxidoreductase subunit I	KU509321	WP_048810348.1	99
nuoJ	NADH-quinone oxidoreductase subunit J	KU509322	WP_048810347.1	99
nuoK	NADH-quinone oxidoreductase subunit K	KU509323	WP_012464548.1	100
nuoL	NADH dehydrogenase subunit L	KU509324	WP_012464547.1	98
nuoM	NADH-quinone oxidoreductase subunit M	KU509325	WP_012464546.1	99
nuoN	NADH dehydrogenase subunit N	KU509326	WP_012464545.1	99
Cytochrome C oxidase and Complex III (ACIII) (40)				
cyoE	protoheme IX farnesyltransferase	KU509378	WP_012463763.1	99
ctaA	cytochrome c oxidase assembly protein subunit 15	KU509379	WP_012463762.1	99
cyoC	cytochrome c oxidase subunit 3	KU509342	WP_012464286.1	99
cyoA	cytochrome c oxidase subunit 2	KU509344	WP_012464280.1	100
cyoB	cytochrome c oxidase subunit 1	KU509341	WP_012464287.1	99
	caa$_3$-type oxidase, subunit IV	KU509343	WP_048810305.1	98
cccA	cytochrome c oxidase, *cbb$_3$*-type, subunit III	KU509340	WP_012464288.1	100
cytC	cytochrome c	KU509481	WP_012463333.1	97
ccoO	cytochrome c oxidase *cbb$_3$*-type subunit 2	KU509339	WP_012464289.1	99
ccoN	cytochrome c oxidase *cbb$_3$*-type subunit 1	KU509338	WP_048810306.1	99
	cytochrome c & quinol oxidase polypeptide I	KU509482	WP_012462607.1	91
	heme/copper-type cytochrome/quinol oxidase, subunit 1	KU509483	WP_012462607.1	99

ActG*	Hypothetical membrane-associated protein	Ga0079954 _121677	WP_012464292.1	99
ActF*	quinol:cytochrome c oxidoreductase quinone-binding subunit 2	KU509337	WP_012464293.1	99
cccA – ActE*	cytochrome c oxidase, cbb₃-type, subunit III	KU509336	WP_012464294.1	99
ActD*	Hypothetical membrane-associated protein	Ga0079954 _121680	WP_012464295.1	100
ActC*	prokaryotic molybdopterin-containing oxidoreductase family, membrane subunit	KU509335	WP_012464296.1	99
hybA – ActB*	prokaryotic molybdopterin-containing oxidoreductase family, iron-sulfur binding subunit	KU509334	WP_012464297.1	99
ActA*	cytochrome c7	KU509333	WP_012464298.1	99
Nitrogen fixation				
nifH	Mo-nitrogenase iron protein subunit NifH	KU509347	WP_012464212.1	99
nifV	homocitrate synthase	KU509346	WP_012464213.1	99
nifD	Mo-nitrogenase MoFe protein subunit NifD precursor	KU509348	WP_012464210.1	99
nifK	Mo-nitrogenase MoFe protein subunit NifK	KU509349	WP_048810527.1	99
nifE	nitrogenase molybdenum-cofactor synthesis protein	KU509350	WP_012464208.1	99
nifN	nitrogenase molybdenum-iron protein NifN	KU509351	WP_048810526.1	99
nifX	nitrogen fixation protein NifX	KU509352	WP_012464206.1	100

756 # nucleotide gene sequences contain nucleotide do not have accession numbers at the time of

757 submission. * Alternative Complex III genes - see reference (40)

758

759

760